Thin Solid Films 535 (2013) 287–290

Contents lists available at SciVerse ScienceDirect

Thin Solid Films

journal homepage: www.elsevier.com/locate/tsf

Application of impedance spectroscopy to investigate the electrical properties around the *pn* interface of $Cu(In,Ga)Se_2$ solar cells

Mutsumi Sugiyama [a,*], Muneatsu Hayashi [a], Chizuru Yamazaki [a], Nafisah Binti Hamidon [a], Yuiko Hirose [a], Masayuki Itagaki [b]

[a] Department of Electrical Engineering, Faculty of Science & Technology, Tokyo University of Science, 2641 Yamazaki, Noda 278-8510, Japan
[b] Department of Pure and Applied Chemistry, Faculty of Science & Technology, Tokyo University of Science, 2641 Yamazaki, Noda 278-8510, Japan

ARTICLE INFO

Available online 7 December 2012

Keywords:
CIGS solar cell
Impedance spectroscopy
pn Interface

ABSTRACT

The application of impedance spectroscopy (IS) analytical theory to the characterization of $Cu(In,Ga)Se_2$ (CIGS)-based solar cells was investigated. The equivalent circuit of the CIGS solar cell consisting of series and parallel resistances and a "capacitance-like element" labeled as constant phase element (CPE) around the CdS/CIGS interface was developed. The CPE reflects the depletion layer thickness and the *pn* interface uniformity and quality. In particular, the CPE-*p* value, which is an index of impedance of CPE, affects the quality around the CdS/CIGS interface in terms of defect existence and inhomogeneity of the heterojunction. These results show possible candidate for the practical application of IS as a simple method for characterizing the heterogeneity of a *pn* interface.

1. Introduction

Chalcopyrite semiconductors, such as $Cu(In,Ga)Se_2$ (CIGS), are used to fabricate thin-film solar cells because of their stability, high conversion efficiency, and relatively low cost. Despite such advantages, the electrical properties of CIGS solar cells have not yet been comprehensively clarified as such cells exhibit a complex composite structure that consists stacked layers of several materials. Although around material interfaces (e.g., *n*-CdS/*p*-CIGS interface) are known to play an important role in carrier transfer/recombination processes and solar cell properties, their influence on device performance remains unclear [1]. Consequently, deep level transient spectroscopy (DLTS) [2–7] and admittance spectroscopy (AS) [7–12] have been applied by several research groups in an attempt to characterize the defect physics around the *pn* interface. These research techniques have also been used to study other semiconductors made from Si and GaAs. For example, Igalson et al. adopted these techniques to investigate the influences of specific electronic properties of defects found in the absorber on the basic parameters of a photovoltaic device [5,7]. Sakurai et al. also utilized these techniques and found that CdS films are necessary for effectively annealing CIGS films, as they prevent chemical reactions at CIGS surfaces [12]. However, these methods are complex for the commercial use. For the engineering viewpoint, rapid and simple technique is very important without sample cooling/heating and appropriate electrodes. Moreover, since the basical AS theory has developed for the case of single *pn* junction or Schottky contact, the appearance of extra diodes and/or Schottky contacts in series with the main junction was not accounted for [8,13]. In fact, owing to the complex nature around the *pn* interface and materials, CIGS solar cells comprise several shunt and series resistances. Accordingly, it is difficult to comprehensively characterize the defects and electrical properties of CIGS semiconductors using only DLTS and AS.

The analytic theory of impedance spectroscopy (IS) is increasingly being applied as an analytical tool [14–16] in chemical-material research and has proved invaluable to electrochemical studies on materials and devices such as fuel cells, rechargeable batteries, and corrosive substances. At present, IS is also commonly used to characterize dye-sensitized solar cells (DSCs) during design and degradation processes [17,18]. To date, however, limited research has been reported for investigating IS for solid-state semiconductor devices including CIGS-based solar cells [19–28]. Further, as the mechanism of IS for solar cells is a complicated phenomenon, little in-depth research on equivalent circuit analysis has been conducted. The impedance data obtained by the IS analysis of DSCs is reflected in the homogeneity, defects, and impedance properties of the TiO_2/dye interface [17,18]. Therefore, applying IS to examine CIGS solar cells is a promising tool for direct observation of the CdS/CIGS interface. Indeed, several complex phenomena that affect the performance of solar cells were observed around the CdS/CIGS interface, including the existence of grain boundaries and defects, diffusion of Cd into CIGS, and band bending around the *pn* interface. Understanding the equivalent circuit of the IS is critical to understanding the scientific principles that influence around interface properties and to ensuring effective engineering of high performance solar cells.

* Corresponding author. Tel./fax: +81 4 7121 1585.
E-mail address: mutsumi@rs.noda.tus.ac.jp (M. Sugiyama).

0040-6090/$ – see front matter © 2012 Elsevier B.V. All rights reserved.
http://dx.doi.org/10.1016/j.tsf.2012.11.070

In this study, utilization of IS is investigated to characterize the impedance properties of CIGS solar cells. First, the equivalent circuit of CIGS solar cells is proposed for IS analysis. Then, the correlation between the impedance properties and equivalent circuit of CIGS solar cells is investigated through observation of impedance variations under dark conditions. Finally, we critically discuss the application of impedance spectroscopy as a simple method for characterizing the heterogeneity around the *pn* interface in CIGS solar cells with different thicknesses of the CdS buffer layer.

2. Experimental detail

Single-phase polycrystalline CIGS ($CuIn_{0.8}Ga_{0.2}Se_2$) films approximately 2.0-μm-thick were prepared by employing a conventional, three-stage process on Mo-coated soda-lime glass. CdS was deposited on CIGS films by chemical bath deposition to form cell structures. Subsequently, undoped ZnO (~100 nm) and n-ZnO:Al transparent conducting oxide (TCO) layers were successively deposited by RF sputtering. Typical efficiencies of the solar cells are about 6–10% (with CdS buffer layer) or less than 1% (without CdS buffer layer) under AM 1.5 and 100 mW/cm^2 illumination. The impedance measurements were carried out using an NF FRA5087 frequency response analyzer with frequencies ranging from 10 Hz to 1 MHz. For all measurements, a 10 mV AC signal was applied to the test device. Measurements were obtained under dark conditions at room temperature. The fitting of the acquired data was performed using Z-plot software.

3. Results and discussion

First, the equivalent circuit of CIGS solar cells for impedance analysis is proposed. In general, an equivalent circuit of simple heterojunction materials consists of three elements, namely, a series resistance (R_s), parallel circuit of parallel resistance (R_p), and constant capacitance (C) or "capacitance-like element" called a constant phase element (CPE). These models are shown in Fig. 1. A CPE is an impedance that displays non-ideal, frequency-dependent properties and a constant phase for over the entire frequency. In general, non-ideal behavior originates from a distribution in the current density due to material inhomogeneity For example, a CPE is often used in DSC impedance models in place of a capacitance-like element to compensate for inhomogeneity in the TiO_2/dye interface [17,18]. The impedance of CPE (Z_{CPE}) is defined by CPE index "*p*" (CPE-*p*) and CPE constant "*T*" (CPE-*T*) as follows;

$$Z_{CPE} = \frac{1}{(j\omega)^p T}. \quad (1)$$

Nyquist plots for each of the equivalent circuits are also shown in Fig. 1. The horizontal axis (real axis) represents the resistance and the normal axis (imaginary axis) represents the capacitance of the equivalent circuit. For the equivalent circuit using C, the diameter of the semicircle represents R_p, and the value of the intersection to the right of the semicircle and the horizontal axis represents R_s, as shown in Fig. 1(a). On the other hand, the Nyquist plot of the equivalent circuit using a CPE makes single semicircles with their centers lying below the imaginary axis, as shown in Fig. 1(b).

Applying these simple models of CIGS solar cells, a typical band diagram and proposed equivalent circuit model of a CIGS solar cell for impedance analysis are shown in Fig. 2. In general, an equivalent circuit of a layered-structure CIGS solar cell has a resistance component of several thin film layers, and an R_p-C or R_p-CPE parallel component around several interfaces. However, C or CPE values obtained by the depletion around CdS/CIGS *pn* interface and ZnO/CdS hetero-interface tend to be larger than those of the other layers and interfaces because the valence and conduction bands around ZnO/CdS/CIGS have a tendency of bending. Therefore, capacitance elements such as C or CPE, except CdS/CIGS and ZnO/CdS interfaces, are negligible. Moreover, impedance properties around the CdS/CIGS interface are affected by applied voltage and frequency as band bending, carrier concentration, and depletion layer thickness around the *pn* interface are changed. In fact, around the CdS/CIGS interface tend to be inhomogeneous because there are many defects and grain boundaries at the CIGS layer around the interface. Therefore, the equivalent circuit around the CdS/CIGS interface is describable by R_p-CPE parallel components. In contrast, there is almost no existence of the depletion layer around the ZnO/CdS interface, and the equivalent circuit around the interface is describable by R_p-C parallel components. In addition, the resistance values of several layers, especially TCO and the CIGS bulk layer, are summarized as R_s. As a result, an equivalent circuit of a CIGS solar cell for impedance analysis is simplified in Fig. 2(b).

Next, experimental results of IS are applied to this calculation model using the proposed equivalent circuit model. Nyquist plots of CIGS solar cells as a function of CdS thickness are shown in Fig. 3(a).

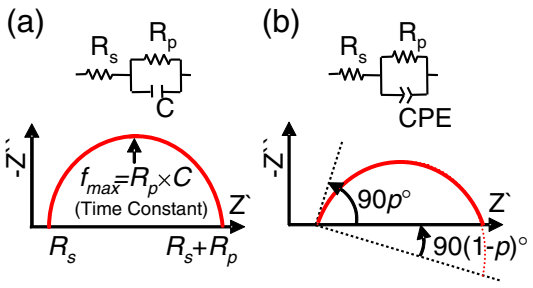

Fig. 1. Equivalent circuits and Nyquist plots of simple heterojunction materials consisting of three elements: R_s, R_p, and (a) C or (b) CPE.

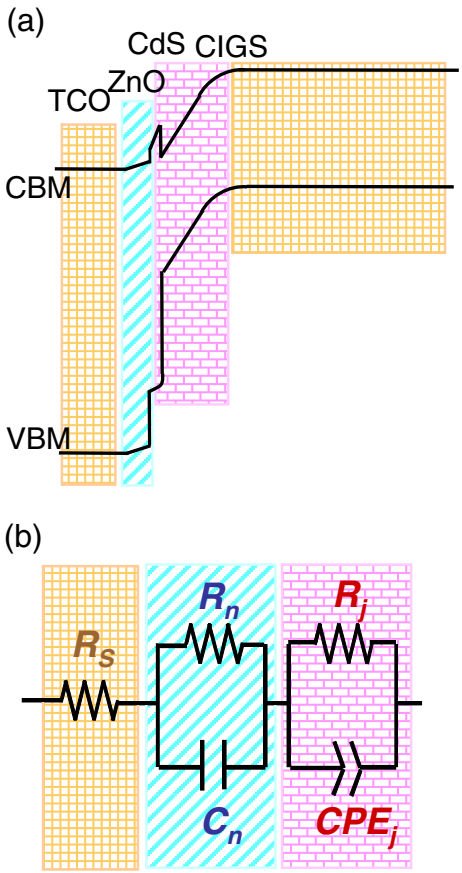

Fig. 2. (a) Representative band alignment of CIGS solar cells and (b) proposed equivalent circuit models of CIGS solar cells for IS.

It is noted that a horizontal axis (real axis) represents the resistance of the solar cell and a normal axis (imaginary axis) represents the capacitance of the solar cell. All of the Nyquist plots made double semicircles with their centers lying below the imaginary axis. The radii of the semicircles tend to increase with increasing CdS thickness. To distinguish two components, Bode plot of the solar cells is also shown in Fig. 3(b). There are two critical frequencies about the order of 10^3 Hz and 10^5 Hz. It is noted that we fitted the obtained data using several types of equivalent using C and CPE. As a result, proposed equivalent was appropriated. These results reflected that there are many inhomogeneity phenomena, such as defects, grain boundaries, Cd diffusion into CIGS layer, and so on, around the CdS/CIGS interface. On the other hand, there are probably small defects and inhomogeneities around the ZnO/CdS interface compared with around the CdS/CIGS interface.

To investigate the effect of the CdS layer, fitted C_j (CPE around the CdS/CIGS interface) and C_n (capacitance around the ZnO/CdS interface) values of the proposed equivalent-circuit parameters are calculated by using the peak frequency of the semicircle (f_{max}) and R of the R_p-C or R_p-CPE parallel component as follows:

$$C_j = T^{\frac{1}{p}} R^{\frac{1-p}{p}} \tag{2}$$

$$C_n = \frac{1}{2\pi R f_{max}}. \tag{3}$$

The obtained values of C_j and C_n as a function of CdS thickness are shown in Fig. 4. The C_j value increases with increasing CdS thickness from 0 nm (without the CdS layer) to 50 nm. This result indicates that depletion layer extended up to the edge of the CdS layer and the C_j value depended on the CdS layer thickness. On the other hand, the C_j value remained constant for CdS thickness from 50 nm to 100 nm because the depletion layer thickness was independent of the CdS layer thickness. In this case, a part of the CdS layer simply served as series resistance of the solar cell. In addition, the C_n value was independent of the CdS layer thickness from 0 nm to 100 nm because the depletion layer did not extend up to the ZnO layer. Judging from typical band structure of CIGS solar cell, balance and conduction bands around ZnO/CdS are also bended. Therefore, an electric field existed around the interface and the interface has a small capacitive element. The experimental result showed that the C_n of ZnO/CdS is smaller by 100 than that of C_j, major capacitive element around CdS/CIGS *pn* interface. These results may be agreed with our proposed model and equivalent circuit. Therefore, using IS, we could conveniently observe the behavior of the depletion layer around the CdS/CIGS interface under dark conditions without sample heating/cooling.

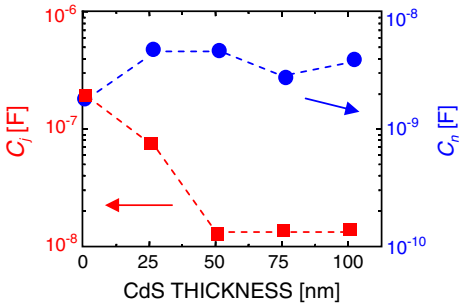

Fig. 4. Proposed equivalent circuit parameters C_j and C_n as functions of CdS thickness.

Finally, inhomogeneity around the CdS/CIGS interface is discussed using CPE-*p* values. The CPE-*p* values of CIGS solar cells as a function of CdS thickness are shown in Fig. 5. The CPE-*p* value increased with increasing CdS thickness from 0 nm (without CdS layer) to 50 nm. On the other hand, the value remained constant in the case of standard CdS thickness from 50 nm to 100 nm. In the case of the impedance model of a DSC solar cell, CPE is often used in place of a capacitance-like element to compensate for inhomogeneity in the TiO_2/dye interface. Judging from this tendency, the CPE-*p* value reflects the ideality of the *pn* interface in semiconductor-based solar cells. The CPE-*p* value equals 1 when an ideal capacitor without defects and/or grain boundary is obtained, and the CPE-*p* value equals 0 when a capacitor element is not obtained due to many defects and/or roughness around the *pn* interface. In other words, the quality of the solar cell, especially around the *pn* interface, is reflected by the proximity of the CPE-*p* value to 1. In this case, IS signals of CIGS solar cells using a thin CdS layer (<50 nm) cause significant defects and/or grain boundaries around the *pn* interface because the CdS layer is not able to cover the entire surface in a homogenous manner. In contrast, for the CIGS solar cells using a thick CdS layer (>50 nm), the number of defects and/or grain boundaries around the *pn* interface tends not

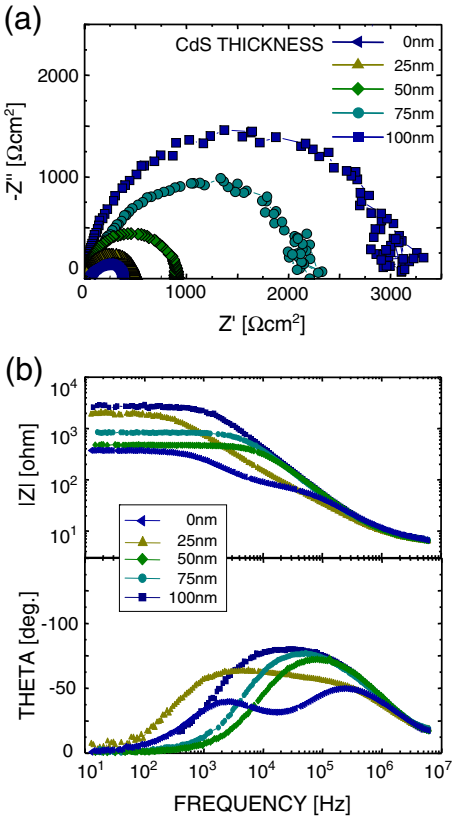

Fig. 3. (a) Nyquist plots and (b) Bode plots (amplitude |Z| and phase θ) of CIGS solar cells as a function of CdS layer thickness.

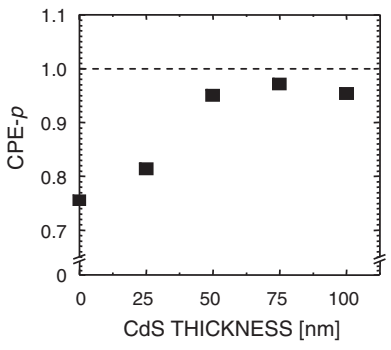

Fig. 5. CPE-*p* of CIGS solar cells as a function of CdS layer thickness.

to change because the surface of the CIGS thin film is covered. The results of this research imply that solar cell quality, especially around the *pn* interface, is reflected in CPE-*p*. Further in-depth investigations are necessary to fully uncover the proper one equivalent circuit of CIGS solar cells. The results of this research show possible candidate towards realizing the practical application of IS as an appropriate method for characterizing the heterogeneity of the *pn* interface.

4. Conclusions

The analytical theory of IS was applied to investigate CIGS solar cells. The equivalent circuit of the CIGS solar cell, which is extremely sensitive to the depletion layer thickness and defect properties around the *pn* interface, was defined. The CPE-*p* value showed an increasing trend with increasing CdS layer thickness when the CdS layer was not very thick. On the other hand, the CPE-*p* value remained constant for appropriate CdS layer thickness. The trend of the CPE-*p* values confirms that the solar cell quality, especially around the *pn* interface, can be reflected very well using IS. Therefore, IS proves to be an appropriate technique for conveniently observing the behavior of the depletion layer around the CdS/CIGS interface under dark conditions without sample heating/cooling.

Acknowledgments

The authors would like to thank Y. Nakano, M. Warasawa, and Y. Matsumoto for their assistance in conducting the experiments. The authors thank Dr. K. Tang and Dr. B. Fan for stimulating discussions. This work was supported in part by Advanced Device Laboratories, Research Center for Green and Safety Sciences, and Photovoltaic Science and Technology Research Division, Research Institute for Science and Technology under Tokyo University of Science.

References

[1] A. Niemegeers, M. Burgelman, R. Herberholz, U. Rau, D. Hariskos, H.W. Schock, Prog. Photovolt. Res. Appl. 6 (1998) 407.
[2] R.K. Ahrenkiel, Solar Cells 16 (1986) 549.
[3] N. Christoforou, J.D. Leslie, S. Damaskinos, Solar Cells 26 (1989) 197.
[4] F.A. Abou-Elfotouh, L.L. Kazmerski, H.R. Moutinho, J.M. Wissel, R.G. Dhere, A.J. Nelson, A.M. Bakry, J. Vac. Sci. Technol. A 9 (1991) 554.
[5] M. Igalson, H.W. Schock, J. Appl. Phys. 80 (1996) 5765.
[6] L.L. Kerr, Sheng S. Li, S.W. Johnston, T.J. Anderson, O.D. Crisalle, W.K. Kim, J. Abushama, R.N. Noufi, Solid State Electron. 48 (2004) 1579.
[7] M. Igalson, C. Platzer-Björkman, Sol. Energy Mater. Sol. Cells 84 (2004) 93.
[8] T. Walter, R. Herberholz, C. Müller, H.W. Schock, J. Appl. Phys. 80 (1996) 4411.
[9] G. Hanna, A. Jasenek, U. Rau, H.W. Schock, Thin Solid Films 387 (2001) 71.
[10] M. Turcu, U. Rau, Thin Solid Films 431–432 (2003) 158.
[11] J.W. Lee, J.D. Cohen, W.N. Shafarman, Thin Solid Films 480–481 (2005) 336.
[12] T. Sakurai, N. Ishida, S. Ishizuka, M.M. Islam, A. Kasai, K. Matsubara, K. Sakurai, A. Yamada, K. Akimoto, S. Niki, Thin Solid Films 516 (2008) 7036.
[13] D.L. Losee, J. Appl. Phys. 46 (1975) 2204.
[14] J.R. Mac Donald, W.B. Johnson, Impedance Spectroscopy, Wiley, New York, 1987.
[15] K.S. Cole, R.H. Cole, J. Chem. Phys. 9 (1941) 341.
[16] K.S. Cole, R.H. Cole, J. Chem. Phys. 10 (1942) 98.
[17] M. Itagaki, K. Hoshino, I. Shitanda, K. Watanabe, J. Power Sources 195 (2010) 6905.
[18] M. Itagaki, Y. Nakano, I. Shitanda, K. Watanabe, Electrochim. Acta 56 (2011) 7975.
[19] M. Lal, P.K. Batham, N. Goyal, Sol. Energy Mater. Sol. Cells 36 (1995) 111.
[20] J.H. Scofield, Sol. Energy Mater. Sol. Cells 37 (1995) 217.
[21] H. Bayhan, A.S. Kavasoğlu, Turk. J. Phys. 27 (2003) 529.
[22] H. Bayhan, A.S. Kavasoğlu, Solar Energy 80 (2006) 1160.
[23] R. Loef, J. Schoonman, A. Goossens, J. Appl. Phys. 102 (2007) 024512.
[24] R. Loef, J. Schoonman, A. Goossens, Sol. Energy Mater. Sol. Cells 92 (2008) 1579.
[25] E. Chassaing, P. Grand, E. Saucedo, A. Etcheberry, D. Lincot, ECS Trans. 19 (2009) 189.
[26] Y. Fu, R. You, K. Lew, J. Electrochem. Soc. 156 (2009) E133.
[27] K. Laes, S. Bereznev, R. Land, A. Tverjanovich, O. Volobujev, R. Traksma, T. Raadik, A. Opik, Energy Procedia 2 (2010) 119.
[28] U. Reislöhner, C. Ronning, Appl. Phys. Lett. 100 (2012) 252111.